Phosphole-based π-conjugated electroluminescent materials for OLEDs†‡

Damien Joly,[a] Denis Tondelier,[b] Valérie Deborde,[a] Bernard Geffroy,*[b] Muriel Hissler*[a] and Régis Réau*[a]

Received (in Montpellier, France) 15th February 2010, Accepted 18th March 2010
DOI: 10.1039/c0nj00122h

Novel mixed phosphole–fluorene π-conjugated systems have been prepared using the Fagan–Nugent route. Their optical (UV-visible absorption, fluorescence spectra) and electrochemical properties have been systematically evaluated. The variation of the substitution pattern of phosphole derivatives and chemical modification of their P atoms afford thermally stable derivatives which are photoluminescent. The use of these derivatives as emitters in OLEDs strongly depends on the substituent linked on the P-atom. The gold complexes are not stable electroluminescent materials since they decompose rapidly when the devices are operating. In contrast, the thiooxophospholes are stable electroluminescent materials, and the OLEDs incorporating these derivatives as emitters display very high performances.

Introduction

The synthesis of new π-conjugated materials with specific electronic and photophysical properties continues to attract considerable attention due to their use as materials for opto-electronic applications such as organic light-emitting diodes (OLEDs) or photovoltaic cells.[1] With this aim, various heterocyclopentadienes (thiophene, pyrrole, silole, *etc.*) have been incorporated into the backbone of π-conjugated systems, since their electronic properties are dependent on the nature of the heteroatom.[1b,2,3] In the last decade, phospholes have emerged as appealing building blocks for the tailoring of π-conjugated systems, since they display electronic properties that are markedly different from those of the widely used highly aromatic thiophene and pyrrole rings.[3] The key property of these P-rings for the molecular engineering of π-conjugated systems is the presence of a reactive phosphorus centre due to the low aromatic character of this P-heterole. In fact, delocalization within the phosphole ring arises from a hyperconjugation involving the exocyclic P–R σ-bond and the π-system of the dienic moiety, leading to σ–π hyperconjugation phenomenon.[4] This specific feature allows straightforward access to a wide range of novel derivatives with diverse optical and electrochemical properties by simple P-chemical modifications. This property of the phosphole ring has been fully exploited by several groups for the tailoring of π-conjugated systems. The first systematic investigation of the optical and the electrochemical properties of phosphole-based conjugated oligomers and polymers was conducted with 2,5-diarylphosphole derivatives **A** (Fig. 1).[5] A variety of other small molecules, including for example linear oligo(phosphole) **B$_{1,2}$**,[6] mixed phosphole–thiophene oligomers **C**[7] or dendritic structures **D**,[8] have been studied by different groups (Fig. 1). Well-defined emissive linear π-conjugated polymers **E** (Fig. 1) incorporating phosphole rings have also been recently reported.[9] Ring-fused π-systems incorporating phosphorus atoms (benzophospholes, dithienophospholes) are not strictly speaking "phosphole" derivatives, since the fused benzene or the thiophene ring remain aromatic to the detriment of the phosphole cycle. These compounds have to be regarded as P-bridged bi(π-systems). However, it is worth noting that these rigid derivatives are generally highly emissive, as illustrated with bisphosphoryl-bridge stilbenes **F**,[10] dithieno-[*b*,*d*]phosphole-based compounds **G**[11] or bithiophene-fused benzo[*c*]phospholes **H**[3a,12] (Fig. 1). As observed for related

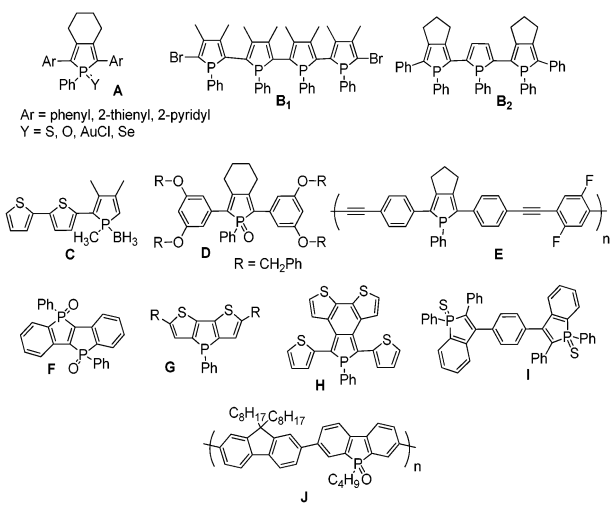

Fig. 1 Representative examples of P-based π-conjugated systems based on phospholes (**A–E**) and fused phospholes (**F–J**).

[a] *Sciences Chimiques de Rennes, UMR 6226 CNRS-Université de Rennes 1, Campus de Beaulieu, 35042 Rennes Cedex, France. E-mail: rreau@univ-rennes1.fr, mhissler@univ-rennes1.fr; Fax: +33 (0)2 23 23 69 39; Tel: +33 (0)2 23 23 57 83*
[b] *CEA/LITEN & LPICM, Ecole Polytechnique, 91128 Palaiseau, France*

† A Pascal. This article is part of a themed issue on Main Group chemistry.

‡ Electronic supplementary information (ESI) available: Other experimental details concerning the new compounds and their related diodes. CCDC reference number 765609. For ESI and crystallographic data in CIF or other electronic format see DOI: 10.1039/c0nj00122h

phosphole-containing materials, their optical and electrochemical properties can be properly tuned by P-chemical modifications.

The study of the derivatives depicted in Fig. 1 has enabled a deep understanding of the fundamental structure–property relationships of phosphole-based π-conjugated systems. The next challenge is clearly to exploit these novel organic materials for the fabrication of optoelectronic devices. Basically, almost all the described P-containing oligomers or polymers (Fig. 1) are potentially suitable materials for OLED applications since (*i*) they are fluorescent, (*ii*) their redox potentials are low enough to allow charges to be injected, and (*iii*) they are thermally stable enough to envisage deposition *via* sublimation. However, there is a gap between having a material exhibiting the expected properties to be used in OLEDs and having a material that can effectively be used in a device. This is due to the fact that light-emission in OLEDs is a consequence of radiative decay of excitons generated by the combination of electrons and holes injection from both electrodes.[13] Therefore, a material has to satisfy a large number of technical requirements to be really efficient as an electroluminescent layer in OLEDs. For example, the conjugated material has (*i*) to give pinhole free homogeneous layer *via vacuum* deposition or spin coating, (*ii*) to be stable under an electric field, (*iii*) to undergo balanced charge carrier injection from both electrodes, (*iv*) to exhibit comparable charge-transporting properties of both electrons and holes to favor exciton formation, and (*v*) to keep its emission behavior in the solid state.[13] Indeed, a compound with high quantum yields and reversible redox processes in solution can be an inefficient material for optoelectronic applications.

Up to now, applications to organic semiconductor devices of P-based materials have remained underdeveloped. It has been recently shown that benzophosphole sulfide **I**[14] (Fig. 1) is an efficient electron-transporting material in OLED, and that copolymers **J**[15] (Fig. 1) incorporating dibenzophosphole subunits are solution-processable materials for single-layer OLEDs. Beside these examples involving fused-derivatives, only phosphole-based oligomers **A** (Fig. 1) have proven to be suitable electroluminescent materials for OLEDs.[5b,e] They have been used in single-layer devices, showing that they can act both as emissive and charge-transporting materials, and also as dopants for the fabrication of efficient white-emitting OLEDs.[5b,e,16] Therefore, there is still a need to really show that phosphole-based π-conjugated systems can satisfy all the diverse criteria to be suitable materials for OLEDs.

In this paper, we describe the synthesis and elucidation of electronic properties following experimental results (UV-vis spectroscopy, electrochemical behavior) of novel mixed phosphole–fluorene π-conjugated systems (Scheme 1). Multilayer OLEDs based on these materials will be described. A comparative study on the influence of the substitution pattern of the 2,5-substituent (fluorenyl *versus* phenyl) and of the phosphorus atom (sulfur *versus* gold) on their electronic property and OLED performances is provided. OLEDs exhibiting the highest external quantum efficiency values ever reached for P-based materials are reported.

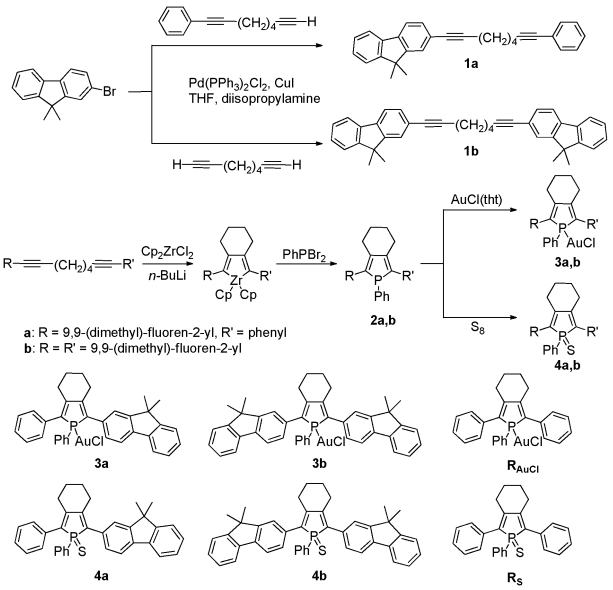

Scheme 1 Synthesis of mixed fluorene–phosphole derivatives.

Synthesis and characterization of mixed fluorene–phosphole derivatives

We have investigated the Fagan–Nugent method,[17] which is a versatile route to 2,5-diarylphospholes **A** (Fig. 1), for the preparation of the target mixed linear fluorene–phosphole derivatives. The diynes **1a,b** were obtained in medium yields (*ca.* 80–60%) *via* Sonogashira coupling of 9,9′-dimethyl-2-bromofluorene with 1-phenyl-octa-1,7-diyne or octa-1,7-diyne, respectively (Scheme 1). Their treatment with "zirconocene", generated *in situ* from Cp_2ZrCl_2 and BuLi (2 equiv.), followed by addition of $PhPBr_2$, afforded the target mixed fluorene–phospholes **2a,b** (Scheme 1). These compounds give usual $^{31}P\{^1H\}$ NMR spectrum (δ (CD_2Cl_2): **2a**, +11.5; **2b**, +12.4).[4,5] They were not isolated since σ^3,λ^3-phosphole derivatives are generally not thermally stable enough to be used as materials for OLEDs.[5e]

Phospholes **2a,b** were transformed into gold complexes **3a,b** and thiooxophospholes **4a,b** by treatment with (tetrahydrothiophene)AuCl and elemental sulfur, respectively (Scheme 1).[5a,e] They were readily purified by column chromatography and isolated as air-stable compounds in good yields (60%–70%, Table 1). They exhibit expected NMR data, and their structures were supported by high-resolution mass spectrometry and elemental analysis. The structure of the gold complex **3b** was determined unambiguously by X-ray crystallography (Fig. 2). The metric data of the phosphole–AuCl subunit compare well with those of other related complexes.[5e,11c] For example, the phosphorus center adopts a distorted tetrahedral geometry (Table 1) with typical P–Au (2.2287(15) Å) and P–C (1.815(6) Å–1.824(7) Å) bond lengths (Table 2). The metal atom displays an almost linear geometry (P–Au–Cl, 175.24°). The angles between the central P-ring and the two fluorenyl substituents are relatively high (56.6° and 56.0°). These twist angles are comparable (43.5° and 54.5°) to those observed for the 2,5-biphenylphosphole complex $\mathbf{R_{AuCl}}$ (Scheme 1).[5e] The shortest distance between two Au-centers is 7.90 Å, indicating

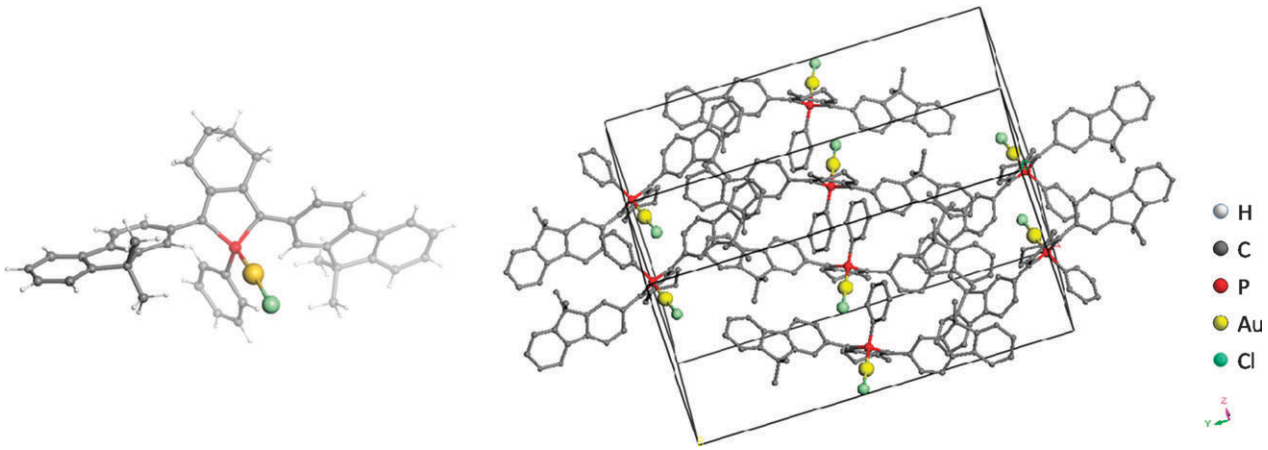

Fig. 2 Molecular structure of phospholes **3b** in the solid state and a perspective view of the packing of gold complex **3b** in the crystalline phase. H atoms are omitted for clarity.

the absence of aurophilic interactions. The intermolecular solid-state organization of the molecule **3b** shows several intermolecular interactions. Firstly, two P-phenyl rings of neighboring molecules π-stacked (3.7 Å) with a parallel-displaced arrangement (Fig. 2). Secondly, T-shape CH···π interactions (*ca.* 2.95 Å) take place between fluorenyl substituents (Fig. 2).

Optical and electrochemical studies

To get an insight into the substitution effect on the optical properties of these novel phosphole-based conjugated systems, their UV-vis absorption and fluorescence spectra were measured in CH_2Cl_2. All phosphole derivatives exhibit an intense absorption band in the UV-visible region attributed to the π–π* transitions of the conjugated system.[5] The values of λ_{max} and the optical end absorption λ_{onset} (the solution optical "HOMO–LUMO" gap) become red-shifted on replacing one or two phenyl groups by fluorenyl substituents (Table 1). These data show an effective π-extension in the present phosphole–fluorene hybrids. It is worth noting that the values of λ_{max} and λ_{em} recorded for **3b**,**4b** are considerably more red-shifted than that of the related *tert*-fluorene (λ_{max} = 348 nm, λ_{em} = 394, 415 nm).[19] This observation is in agreement with theoretical studies predicting that heterocyclopentadienes with a low aromatic character are optimal building blocks for the synthesis of extended π-conjugated systems with a low HOMO–LUMO gap.[2e,3f–h,4c,d] As observed with 2,5-diphenylphosphole derivatives $\mathbf{R_{AuCl}}$, $\mathbf{R_S}$ (Scheme 1), the nature of the P-substituent (sulfur atom or AuCl fragment) has little impact on the maximum of absorption (**3a**/**4a**, **3b**/**4b**, Table 1). σ^4-Phospholes **3a,b** and **4a,b** are fluorophores with broad emissions and their emission maxima depend mainly on the nature of the 2,5-substituents. A yellow–green emission is observed for the 2,5-di(9,9′-dimethylfluorenyl)phospholes **3b**,**4b** (λ_{em} = 560–565 nm), whereas the emission of 2-(9,9′-dimethylfluorenyl)-5-(phenyl)phospholes **3a**,**4a** are blue-shifted ($\Delta\lambda_{em}$ = 40 nm) (Table 1, Fig. 3). The Stokes shifts of the mono-(fluorenyl)phospholes **3a**,**4a** (*ca.* 7578 cm^{-1}) are smaller than those of the bis(fluorenyl)phospholes **3b**,**4b** (*ca.* 7850 cm^{-1}) (Table 1). These Stokes shifts are relatively important (Fig. 3, Table 1), suggesting an important rearrangement of these molecules upon photoexcitation. Remarkably, the nature of

Table 2 Selected bond lengths (Å) and twist angles (°) between the phosphole ring and its 2- and 5-substituents for the gold complex **3b**

Bond length		Angle	
P–(C1)	1.824(7)	(C1)–P–(C8)	93.2(3)
(C1)–C2)	1.351(8)	(C1)–P–(C39)	108.6(3)
(C2)–(C7)	1.472(9)	C(1)–P–Au	117.9(2)
(C7)–(C8)	1.369(9)	(C8)–P–(C39)	106.6(3)
(C8)–P	1.815(6)	C(8)–P–Au	118.11(19)
P–Au	2.2287(15)	C(39)–P–Au	110.8(2)
Au–Cl	2.2934(15)	P–Au–Cl	175.27(5)
Twist angles	56.6/56.0		

Table 1 Optical and electrochemical data for derivatives **3a,b**, **4a,b** and reference compounds $\mathbf{R_{AuCl}}$/$\mathbf{R_S}$

	δ $^{31}P\{^1H\}$/ppm [a]	Yield/%	λ_{abs}/nm [b]	λ_{onset}/nm [b]	ε_{max}/M^{-1} cm^{-1}	λ_{em}/nm [c]	$\phi_f \times 100$ [d]	λ_{em}/nm [e]	$\Phi_f \times 100$ [f]	Ep_a/V [g]	Ep_c/V [g]
3a	41.0	70	373	447	11 700	520	3	518	12	+0.97[h]	−2.05
3b	41.2	70	387	460	18 200	560	70	550	26	+0.87[h]	−2.08
4a	54.0	60	373	450	15 000	520	0.7	520	13	+0.88	−2.10[h]
4b	54.9	64	392	470	11 600	565	3	552	40	+0.82	−2.06[h]
$\mathbf{R_{AuCl}}$ [5e]	41.7	77	358	413	6300	506	7.3	505/630	11.2	+1.45	−2.14
$\mathbf{R_S}$ [5e]	55.3	87	380	440	13 500	516	0.05	517	0.5	+1.12	−2.08[h]

[a] Measured in CD_2Cl_2. [b] Measured in CH_2Cl_2 (5×10^{-5} M). [c] Measured in CH_2Cl_2 (5×10^{-6} M). [d] Measured relative to quinine sulfate (H_2SO_4, 0.1 M). [e] In neat film. [f] Measured in integrating sphere.[18] [g] All potentials were obtained during cyclic voltametric investigations in 0.2 M Bu_4NPF_6 in CH_2Cl_2. Platinum electrode diameter 1 mm, sweep rate: 200 mV s^{-1}. All reported potentials are referenced to the reversible formal potential of the ferrocene/ferrocenium couple. [h] Reversible process.

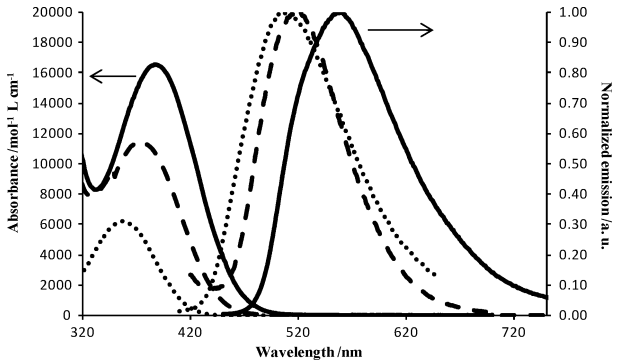

Fig. 3 Absorption spectra and emission spectra of $\mathbf{R_{AuCl}}$ (dotted line), **3a** (dashed line), **3b** (continous line) in CH_2Cl_2.

the P-chemical modification (S/AuCl) has a deep impact on their photoluminescence (PL) quantum yield.

The quantum yields (Φ_f) of the gold complexes are higher than those of the corresponding sulfur derivatives (**3a**/**4a**, **3b**/**4b**, Table 1). In fact the thioxophosphole **4a** is only weakly fluorescent (Φ_f = 0.7%), whereas the emission efficiency of complex **3b** (Φ_f = 70%) is the highest ever recorded for a non-rigidified (*i.e.* "non-fused phospholes", Fig. 1) phosphole derivative. These data recorded in solution suggest that the gold complexes **3a,b** are the most promising materials for the fabrication of OLEDs among the newly prepared mixed phosphole–fluorene derivatives (Scheme 1).

The gold complexes **3a,b** and the thiooxophospholes **4a,b** are thermally stable enough to give thin films upon vacuum sublimation. The absorption and emission spectra recorded in thin films are essentially comparable to those obtained in CH_2Cl_2 solution (Table 1, Fig. 3). It is noteworthy that the gold complexes **3a,b** display one single emission band only in the solid state. This behavior is different from that of the corresponding complex $\mathbf{R_{AuCl}}$ that exhibit dual emission in thin film arising from aggregate formation due to π–π stacking and/or Au–Au interactions. It is very likely that the bulkiness of the fluorene substituents of complexes **3a,b**, and especially the presence of two methyl groups at the 9,9′-positions, prevents the formation of strong aggregates in the solid state. The solid-state PL quantum efficiencies were measured with a calibrated integration sphere system.[18] They vary from 12% (**3a**) to 46% (**4b**) and are notably higher than those of their corresponding all phenyl analogues $\mathbf{R_{AuCl}}$, $\mathbf{R_S}$ (Table 1). Note that the quantum efficiencies are higher in thin film than in dilute solution except for **3b** (Table 1). This behavior is quite rare, because organic fluorophores are generally less emissive in the solid state than in solution due to the formation of less emissive aggregates such as excimers. However, this behavior, which has already been observed for other silole- and phosphole-based π-conjugated systems, is probably due to the steric protection provided by the tetrahedral Si- or P-centers, which precludes the π-stacking of these heavy heteroatom-based chromophores.[8,20] The most important piece of information is that all newly prepared derivatives display good photoluminescence efficiency in the solid state and thus appear to be good candidates as materials for OLEDs. Note that, in contrast to what is observed in solution, the thiooxophosphole derivative **4b** exhibits the highest PL quantum efficiency in thin films (Table 1).

In order to estimate the electrochemical properties of these novel phosphole-based conjugated systems, their redox potentials were determined by cyclic voltammetry (CV). The measurement conditions are summarized in the caption of Table 1. The gold complexes and sulfur derivatives exhibit very different electrochemical behaviour. Reversible oxidation processes take place for the gold complexes **3a,b** only, whereas reversible reduction processes are recorded for the thio-oxophospholes **4a,b** only. These data illustrate the dramatic impact of the nature of the P-chemical modification on the electrochemical properties of phosphole-based π-conjugated systems. Replacing the phenyl rings by fluorenyl substituents at the 2,5-positions of the phosphole ring does not affect the reduction potentials but results in a shift of the oxidation potentials to the negative direction ($\mathbf{R_{AuCl}}$/**3a**/**4a** and $\mathbf{R_S}$/**3b**/**4b** series, Table 1). In line with the conclusions drawn from the UV-vis measurement (*vide supra*) these electrochemical data indicate that the HOMO–LUMO gaps of **3b**,**4b** (**3b**, ΔE = 2.65 V; **4b**, ΔE = 2.64 V) are smaller than those of **3a**,**4a** (**3a**, ΔE = 2.73 V; **4a**, ΔE = 2.79 V) and $\mathbf{R_{AuCl}}$/$\mathbf{R_S}$ ($\mathbf{R_{AuCl}}$, ΔE = 3.0 V; $\mathbf{R_S}$, ΔE = 2.98 V).

OLEDs based on electroluminescent mixed fluorene–phosphole derivatives

Following the study of their optical and electrochemical properties, phosphole derivatives **3a,b** and **4a,b** (Scheme 1) were investigated as organic materials in OLEDs having an tin indium oxide (ITO) anode and an aluminium cathode (Fig. 4, left). The HOMO and LUMO energies for **3a,b** and **4a,b**, estimated from the redox data using a SCE energy level of 4.4 V relative to vacuum,[5e,21] showed rather large barriers for electron injection for phosphole-based materials (Φ_c (4.10) – EA ≈ 1.3–1.1 eV). The barriers for hole injection are lower (Φ_a (5.10) – IP ≈ 0.4–0.6 eV), indicating an unbalanced carrier injection. Therefore, it was necessary to employ a multilayer OLED structure in order to reduce barriers for carrier injection. For such purpose, a series of electron- (Alq_3/BCP/DPVBi) and hole- (CuPc/α-NPB) transport materials were used (Fig. 4, right; Fig. 5). BCP also acts as a hole-blocking layer to avoid emission from Alq_3. Indeed, the investigated OLEDs **I–VI** (Table 3) have an (ITO)/CuPc(10 nm)/α-NPB(50 nm)/organic layer(15 nm)/DPVBi (35 nm)/BCP(10 nm)/Alq_3(10 nm)/LiF(1.2 nm)/Al(100 nm) configuration (Fig. 4 and 5).

The electroluminescence (EL) spectra of the devices resemble the solution and thin-film PL of the mixed fluorene–phosphole derivatives, showing that the EL emission bands are from these P-luminophores. As expected from the thin film study, no low-energy emission arising from excimers is observed. The turn-on voltages required to obtain EL with the gold complexes **3a,b** are relatively high (10.0–11.3 V). The brightness and maximum external quantum efficiency (EQE, η) are superior to those recorded using the reference complex $\mathbf{R_{AuCl}}$ (Devices **I**,**II**/**V**, Table 3). However, these performances are very modest compared to the state of the art. For example, EQEs of 2–4% can be attained with fluorescent materials

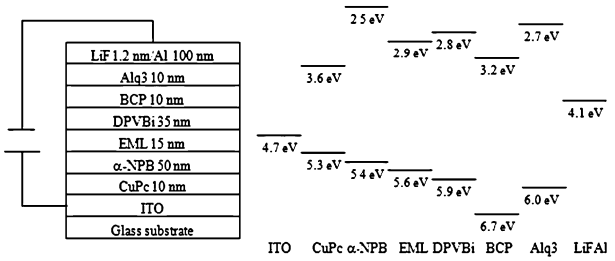

Fig. 4 Structure of the multi-layer OLEDs using fluorene–phosphole derivatives as emissive layer (EML) and energy level HOMO and LUMO diagram.

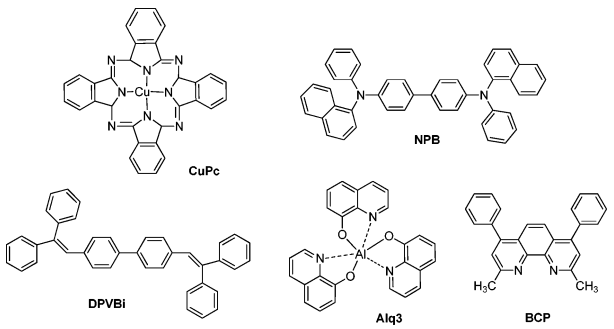

Fig. 5 Chemical structures of the OLED components.

(5% is generally accepted as the upper value that can be reached using electrofluorescent materials). Furthermore, the lifetime of these devices is extremely short. After few seconds, a new red-shifted emission is observed. The intensity of this band increases much faster than the original emission of the gold complex (Fig. 6), modifying strongly the emission of diode. It is very likely that this behavior is due to a fast decomposition of the phosphole gold complexes when an electric field is applied. Indeed, although complexes **3a,b** display high PL efficiency both in solution and thin film (Table 1), they appear not to be valuable EL materials for the fabrication of OLEDs.

The devices **III** and **IV** fabricated with the thioxophosphole derivatives **4a,b** (Table 3) exhibit improved performances. The operating voltages are quite low (4.3–6.3 V) and the brightness is much higher than those observed with the gold complexes (Table 3). As observed for the optical properties in solution and in thin films, the nature of 2,5-substituents modifies the λ_{max}^{EL} and the CIE coordinates (Table 1 and 2) of the OLED.

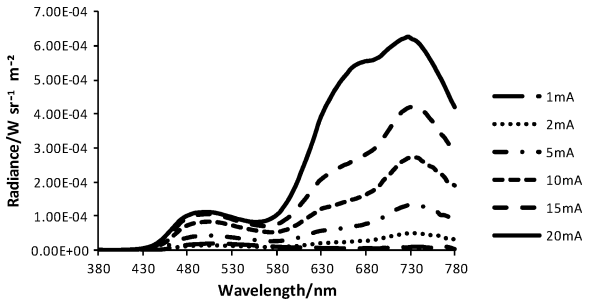

Fig. 6 Emission spectra of the diode **II** depending on applied current.

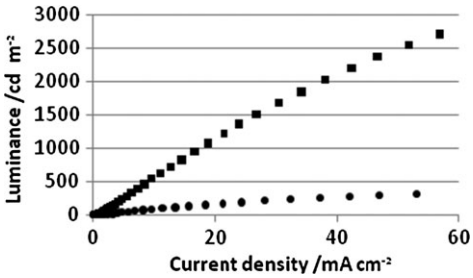

Fig. 7 Luminance–current density characteristics of the diodes **III** (●) and **IV** (■).

Moreover, the brightness of these OLEDs increases linearly with the current density, showing the operational stability of these devices (Fig. 7). The relatively high value of brightness reached with bis(fluorene)phosphole derivative **4b** (device **IV**, Table 3) is noteworthy. This device is the most efficient OLED based on phosphole-based EL materials reported to date. The EQE and power efficiency are good for such a simple device structure and compare well with those recorded with other optimized emissive materials. This result is of particular interest to show that phospholes are useful synthons for the tailoring of EL materials.

Conclusions

In conclusion, we have prepared a novel series of phosphole-based π-conjugated systems bearing fluorenyl substituents. Their electronic properties have been studied both in solution and in the solid state. These new P-derivatives have been used as electroluminescent materials in OLEDs. The gold complexes,

Table 3 EL performance of the multi-layer OLED devices incorporating fluorine–phosphole derivative as emissive layer (se Fig. 4)

								CIE coordinates [b]	
Diode	Sample	λ_{max}^{EL}/nm	V_{on}/V [a]	V_{20}/V [b]	B_{20}/cd m^{-2} [b]	η_{20}/% [b]	Power efficiency/lm W_{20}^{-1} [b]	x	y
I [c]	**3a**	660	10.0	16.9	16.8	0.1	0.02	0.49	0.37
II [c]	**3b**	730	11.3	16.5	4.9	0.1	0.01	0.42	0.41
III [c]	**4a**	524	6.3	11.7	167	0.3	0.2	0.31	0.48
IV [c]	**4b**	560	4.3	10.7	1000	1.8	1.4	0.43	0.53
V [d]	$\mathbf{R_{AuCl}}$	637	9.0	12.0	0.5	0.04	7.5×10^{-3}	—	—
VI [d]	$\mathbf{R_S}$	567	3.2	9.2	26.6	0.05	0.05	—	—

[a] Turn-on voltage at which emission becomes detectable (0.1 cd m^{-2}). [b] Mesured at 20 mA cm^{-2}. [c] Device configurations (thickness): (ITO)/CuPc(10 nm)/α-NPB(50 nm)/organic layer(15 nm)/DPVBi(35 nm)/BCP(10 nm)/Alq_3(10 nm)/LiF(1.2 nm)/Al(100 nm). [d] Device configurations (thickness): ITO/PEDOT:PSS(25 nm)/organic layer(20 nm)/Mg:Ag(80 nm)/Ag(150 nm).[5e]

although they display high fluorescence efficiency, are not interesting materials since they decompose rapidly when the devices are operating. In contrast, thiooxophospholes are stable electroluminescent materials, and the performance of the OLED **IV** fabricated with the bis(fluorenyl)phosphole derivative **4b** is the best ever reported for devices using EL phosphorus-based materials.

Experimental section

General

Details of the X-ray crystallography study. Single crystals suitable for X-ray crystal analysis were obtained by slow evaporation of a dichloromethane solution of **3b**. Single-crystal data collection were performed at 100 K with an APEX II Bruker-AXS (Centre de Diffractométrie, Université de Rennes 1, France) with Mo-Kα radiation (λ = 0.71073 Å).‡ Reflections were indexed, Lorentz-polarization-corrected and integrated by the DENZO program of the KappaCCD software package. The data merging process was performed using the SCALEPACK program.[22] Structure determinations were performed by direct methods with the solving program SIR97,[23] which revealed all the non-hydrogen atoms. The SHELXL program[24] was used to refine the structures by full-matrix least-squares based on F^2. All non-hydrogen atoms were refined with anisotropic displacement parameters. Hydrogen atoms were included in idealized positions and refined with isotropic displacement parameters. Atomic scattering factors for all atoms were taken from International Tables for X-ray Crystallography.[25] In the case of the derivative **3b** a CH_2Cl_2 molecule was found highly disordered in an asymmetric unit. A modelling of its disorder was not possible, and so the protons of this CH_2Cl_2 molecule were not modelled, and we used a 'squeeze' treatment in order to remove the scattering contribution of these molecules which cannot be satisfactorily modelled after this 'squeeze' treatment. Anisotropic displacement parameters associated to the atoms of the derivative **3b** are always satisfactory, and lends confidence to the treatment of the structural resolution of this derivative. Table S1‡ gives the crystallographic data for the derivative **3b** after this 'squeeze' treatment. Table S2‡ gives the crystallographic data for the derivative **3b** before the 'squeeze' treatment. Details of crystal data and structural refinements are given in Table 2.

Syntheses. All experiments were performed under an atmosphere of dry argon using standard Schlenk techniques. Column chromatography was performed in air, unless stated in the text. Solvents were freshly distilled under argon from sodium/benzophenone (tetrahydrofuran, diethyl ether) or from phosphorus pentoxide (pentane, dichloromethane). Cp_2ZrCl_2 was obtained from Alfa Aesar Chem. Co. [$PdCl_2(PPh_3)_2$], CuI, octa-1,7-diyne, *n*-BuLi, diisopropylamine, and S_8 were obtained from Acros Chem. Co. All compounds were used as received without further purification. $PPhBr_2$,[26] 9,9′-dimethyl-2-bromofluorene,[27] AuCl(tht)[28] and 1-phenyl-octa-1,7-diyne[29] were prepared as described in the literature. Preparative separations were performed by gravity column chromatography on basic alumina (Aldrich, Type 5016A, 150 mesh, 58 Å) or silica gel (Merck Geduran 60, 0.063–0.200 mm) in 3.5–20 cm columns. ^{1}H, ^{13}C, and ^{31}P NMR spectra were recorded on Bruker AM300 or DPX200. ^{1}H and ^{13}C NMR chemical shifts were reported in parts per million (ppm) relative to $Si(CH_3)_4$ as external standard. ^{31}P NMR downfield chemical shifts were expressed with a positive sign, in ppm, relative to external 85% H_3PO_4. Assignment of proton atoms is based on COSY experiment. Assignment of carbon atoms is based on HMBC, HMQC and DEPT-135 experiments. High-resolution mass spectra were obtained on a Varian MAT 311, Waters Q-TOF 2 or a ZabSpec TOF Micromass instrument at CRMPO, University of Rennes 1. Elemental analyses were performed by the CRMPO, University of Rennes 1.

Determination of optical data. UV-Visible spectra were recorded at room temperature on a UVIKON 942 spectrophotometer and luminescence spectra were recorded in freshly distilled solvents at room temperature with a PTI spectrofluorimeter (PTI-814 PDS, MD 5020, LPS 220B) using a xenon lamp. Quantum yields were calculated relative to quinine sulfate (Φ = 0.546 in 1 N H_2SO_4).[30]

Cyclic voltammetry measurements. The electrochemical studies were carried out under argon using an Eco Chemie Autolab PGSTAT 30 potentiostat for cyclic voltammetry with the three-electrode configuration: the working electrode was a platinum disk, the reference electrode was a saturated calomel electrode and the counter-electrode a platinum wire. All potential were internally referenced to the ferrocene/ferrocenium couple. For the measurements, concentrations of 10^{-3} M of the electroactive species were used in freshly distilled and degassed dichloromethane (Lichrosolv, Merck) and 0.2 M tetrabutylammonium hexafluorophosphate (TBAHFP, Fluka) which was twice recrystallized from ethanol and dried *in vacuo* prior to use.

Device fabrication and characterization. EL devices based on a multilayer structure were fabricated onto patterned ITO-coated glass substrates from Asahi (sheet resistance 10 Ω m^{-1}) or PGO CEC020S (thickness: 100 nm and sheet resistance: less of 20 Ω m^{-1}). The organic materials (from Aldrich and Syntec) were deposited onto the ITO anode by sublimation under high vacuum ($<10^{-6}$ Torr) at a rate of 0.2–0.3 nm s^{-1}. The common structure of all the devices is the following: a thin layer (10 nm thick) of copper phtalocyanine (CuPc) is used as the hole-injection layer (HIL) and 50 nm of *N*,*N*′-diphenyl-*N*,*N*′-bis(1-naphthylphenyl)-1,1′-biphenyl-4,4′-diamine (α-NPB) as hole-transporting layer (HTL). The emitting layer consists of phosphole derivatives (15 nm). A thin layer of 4,4′-bis(2,2′-diphenylvinyl)biphenyl (DPVBi) (35 nm), a commercially available molecule (from Syntec) is used as electron-transporting layer (ETL). A thin layer of bathocuproine (BCP) (10 nm) is used as hole-blocking layer. Alq_3 (10 nm) is used as electron-transporting layer (ETL). Finally, a cathode consisting of 1.2 nm of LiF capped with 100 nm of Al is deposited onto the organic stack. The entire device is fabricated in the same run without breaking the vacuum. In this study, the thicknesses of the different organic layers were kept constant

for all the devices. The active area of the devices defined by the overlap of the ITO anode and the metallic cathode was 0.3 cm^2.

The current–voltage–luminance (*I–V–L*) characteristics of the devices were measured with a regulated power supply (ACT100 Fontaine) combined with a multimeter and a 1 cm^2 area silicon calibrated photodiode (Hamamatsu). The spectral emission was recorded with a SpectraScan PR650 spectrophotometer. All the measurements were performed at room temperature and at ambient atmosphere with no further encapsulation of devices.

1-(9,9-Dimethylfluoren-2-yl)-8-phenyl-octa-1,7-diyne 1a

Catalytic amounts of $[PdCl_2(PPh_3)_2]$ (99 mg, 0.14 mmol) and CuI (27 mg, 0.14 mmol) were added to a solution of 1-phenyl-octa-1,7-diyne (519 mg, 2.8 mmol) and 9,9′-dimethyl-2-bromofluorene (786 mg, 2.9 mmol) in THF (30 mL) and diisopropylamine (30 mL) at 55 °C. The heterogeneous brown mixture was stirred for 1 day at 55 °C. All volatile materials were removed *in vacuo* and the residue was extracted with diethyl ether (3 × 20 mL). After purification by column chromatography on silica gel (heptane–ethyl acetate, 95:5, v/v, R_f = 0.1) the product **1a** was obtained as a yellow oil (yield 68%, 750 mg, 2.00 mmol). ^{1}H NMR (300 MHz, $CDCl_3$): δ = 7.74 (m, 1H, C$H_{fluorenyl}$), 7.68 (m, 1H, C$H_{fluorenyl}$), 7.56 (m, 1H, C$H_{fluorenyl}$), 7.50–7.40 (m, 4H, 2 CH_{phenyl}, 2 C$H_{fluorenyl}$), 7.40–7.30 (m, 5H, 3 CH_{phenyl}, 2 C$H_{fluorenyl}$), 2.57 (m, 4H, $\equiv$CCH_2), 1.89 (m, 4H, CH_2), 1.53 (s, 6H, CH_3). ^{13}C NMR (75 MHz, $CDCl_3$): δ = 153.9 (s, $C_{fluorenyl}$), 153.5 (s, $C_{fluorenyl}$), 138.8 (s, $C_{fluorenyl}$), 138.7 (s, $C_{fluorenyl}$), 131.6 (s, C$H_{ortho\text{-}phenyl}$), 130.7 (s, C$H_{fluorenyl}$), 128.2 (s, C$H_{meta\text{-}phenyl}$), 127.6 (s, C$H_{fluorenyl}$), 127.5 (s, C$H_{fluorenyl}$), 127.1 (s, C$H_{fluorenyl}$), 125.9 (s, C$H_{para\text{-}phenyl}$), 124.0 (s, $C_{ipso\ phenyl}$), 122.6 (s, C$H_{fluorenyl}$), 122.5 (s, $C_{2\text{-}fluorenyl}$), 120.2 (s, C$H_{fluorenyl}$), 119.9 (s, C$H_{fluorenyl}$), 89.9 (s, $C\equiv$CC_{phenyl}), 89.8 (s, $C\equiv$C$C_{fluorenyl}$), 81.7 (s, C$\equiv$C$C_{fluorenyl}$), 81.0 (s, $\equiv$CC_{phenyl}), 46.8 (s, $C_{9fluorenyl}$), 28.1 (s, $\equiv$CCH_2), 28.0 (s, $\equiv$CCH_2), 27.1 (s, CH_3), 19.2 (s, CH_2), 19.1 (s, CH_2). Anal. calc. for $C_{29}H_{26}$ (374.527): C, 93.00; H, 7.00; Found: C, 93.23; H, 7.15.

1,8-Bis(9,9′-di(methyl)fluoren-2-yl)octa-1,7-diyne 1b

Catalytic amounts of $[PdCl_2(PPh_3)_2]$ (0.35 g, 0.50 mmol) and CuI (0.10 g, 0.50 mmol) were added to a solution of 1,7-octadiyne (0.64 mL, 5.00 mmol) and 9,9′-dimethyl-2-bromofluorene (2.63 g, 10.00 mmol) in THF (20 mL) and diisopropylamine (50 mL) at 55 °C. The heterogeneous brown mixture was stirred for a week at 55 °C. All volatile materials were removed *in vacuo* and the residue was extracted with diethyl ether (3 × 20 mL). After purification by column chromatography on silica gel (heptane–ether, 99:1, v/v, R_f 0.50) the product **1b** was obtained as a pale yellow solid (yield 80%, 3.70 g, 4.00 mmol). ^{1}H NMR (200 MHz, CD_2Cl_2): δ = 7.77–7.72 (m, 2H, C$H_{fluorenyl}$), 7.72–7.66 (m, 2H, C$H_{fluorenyl}$), 7.55–7.51 (m, 2H, C$H_{fluorenyl}$), 7.51–7.46 (m, 2H, C$H_{fluorenyl}$), 7.46–7.39 (m, 2H, C$H_{fluorenyl}$), 7.39–7.32 (m, 4H, C$H_{fluorenyl}$), 2.58 (s, 4H, $\equiv$CCH_2), 1.88 (s, 4H, $\equiv$CCH$_2$CH_2), 1.50 (s, 12H, CH_3). ^{13}C–{^{1}H} NMR (50 MHz, CD_2Cl_2): δ = 153.9 ($C_{fluorenyl}$), 153.6 (s, $C_{fluorenyl}$), 138.7 (s, $C_{fluorenyl}$), 138.5 (s, $C_{fluorenyl}$), 130.5 (s, C$H_{fluorenyl}$), 127.5 (s, C$H_{fluorenyl}$), 127.0 (s, C$H_{fluorenyl}$), 125.8 (s, C$H_{fluorenyl}$), 122.6 (s, C$H_{fluorenyl}$), 122.6 (s, $C_{2fluorenyl}$), 120.1 (s, C$H_{fluorenyl}$), 119.8 (s, C$H_{fluorenyl}$), 89.9 (s, C$_{fluorenyl}$C$\equiv$C), 81.4 (s, C$_{fluorenyl}$C$\equiv$), 46.8 (s, $C_{9\text{-}fluorenyl}$), 28.1 (s, $\equiv$CCH_2), 26.8 (s, CH_3), 19.0 (s, CH_2). MS (LSIMS): *m*/*z* 490.2634 (calculated: 490.26605, $M^{+\bullet}$).). Anal. calc. for $C_{38}H_{34}$ (490.691): C, 93.02; H, 6.98; Found C, 93.36; H, 7.21

1-Phenyl-2-(9,9′-dimethylfluorene-2-yl)-5-(phenyl)phosphole AuCl 3a

To a THF solution (10 mL) of Cp_2ZrCl_2 (286 mg, 1.00 mmol) and 1,8-bis(9,9′-di(methyl)fluorene-2-yl)-octa-1,7-diyne **1a** (366 mg, 1.00 mmol) was added dropwise (*ca.* 1 min), at −78 °C, a hexane solution of *n*-BuLi (2.5 M, 0.8 ml, 2.05 mmol). The solution was warmed to room temperature, and stirred overnight. To this solution was added, at −78 °C, freshly distilled $PhPBr_2$ (0.22 mL, 1.05 mmol). The solution was allowed to warm to room temperature and stirred for 30 h. The solution was filtered on basic alumina (THF) and the volatile materials were removed *in vacuo*. The yellow precipitate of phosphole **2a** (^{31}P{^{1}H} NMR (80 MHz, $CDCl_3$): δ = +11.5) was dissolved in THF (20 mL) and AuCl(tht) (320 mg, 1.00 mmol) was added to the THF solution and stirred at room temperature overnight. The solvent was removed *in vacuo*. After purification by column chromatography on silica gel (*n*-heptane–ethyl acetate, 6:4, R_f = 0.3) the compound **3a** was obtained as a yellow solid (yield 70%, 500 mg, 0.7 mmol). ^{1}H NMR (300 MHz, $CDCl_3$): δ = 7.76–7.30 (m, 17H, 7 C$H_{fluorenyl}$, 2 CH_{ortho}-phenyl, 2 CH_{meta}-phenyl, C$H_{para\text{-}phenyl}$, 5 CH_{phenyl}), 3.10–2.75 (m, 4H, C$_\beta$CH_2), 1.95–1.75 (m, 4H, CH_2), 1.49 (s, 3H, CH_3), 1.45 (s, 3H, CH_3). ^{13}C NMR (50 MHz, $CDCl_3$): δ = 154.0 (s, $C_{fluorenyl}$), 153.9 (s, $C_{fluorenyl}$), 151.1 (d, ^2J(P,C) = 17.4 Hz, C_β), 150.0 (d, ^2J(P,C) = 17.8 Hz, C_β), 139.1 (s, $C_{fluorenyl}$), 138.4 (s, $C_{fluorenyl}$), 134.6 (d, ^1J(P,C) = 58.6 Hz, C_α), 134.0 (d, ^3J(P,C) = 13.8 Hz, CH_{ortho}-phenyl), 132.9 (d, ^2J(P,C) = 13.7 Hz, $C_{fluorenyl}$), 131.7 (d, ^1J(P,C) = 2.7 Hz, CH_{para}-phenyl), 131.6 (d, ^2J(P,C) = 13.7 Hz, C_{phenyl}), 129.4 (d, ^3J(P,C) = 6.2 Hz, C$H_{fluorenyl}$), 129.3 (d, ^{3}J(P,C) = 12.2 Hz, CH_{meta}-phenyl), 128.3 (s, CH_{phenyl}), 128.3 (d, ^2J(P,C) = 6.4 Hz, CH_{phenyl}), 128.0 (s, CH_{phenyl}), 127.7 (s, C$H_{fluorenyl}$), 127.1 (s, C$H_{fluorenyl}$), 125.1 (d, ^1J(P,C) = 58.3 Hz, C_{ipso}), 123.8 (d, ^3J(P,C) = 6.4 Hz, C$H_{fluorenyl}$), 122.7 (s, C$H_{fluorenyl}$), 120.2 (s, C$H_{fluorenyl}$), 120.0 (s, C$H_{fluorenyl}$), 46.8 (s, $C_{9\text{-}fluorenyl}$), 28.5 (d, ^3J(P,C) = 6.6 Hz, C$_\beta$CH_2), 28.3 (d, ^3J(P,C) = 6.6 Hz, C$_\beta$CH_2), 26.8 (s, 2 CH_3), 22.6 (s, CH_2), 22.5 (s, CH_2). ^{31}P{^{1}H} NMR (121 MHz, CD_2Cl_2): δ = 41.00 ppm. MS (ESI): *m*/*z* 737.14152 (calculated 737.1422 $[M + Na]^+$). Anal. calc. for $C_{35}H_{31}PAuCl$ (715.027): C, 58.79; H, 4.37; P, 4.33; Found: C, 58.86; H, 4.59; P, 4.68.

1-Phenyl-2,5-bis(9,9′-di(methyl)fluoren-2-yl)phosphole)AuCl 3b

To a THF solution (10 mL) of Cp_2ZrCl_2 (155 mg, 0.53 mmol) and 1,8-bis(9,9′-di(methyl)fluorene-2-yl)1,7-octadiyne **1b** (469 mg, 0.53 mmol) was added dropwise (*ca.* 1 min), at −78 °C, a hexane solution of *n*-BuLi (2.5 M, 0.42 mL, 1.06 mmol). The solution was warmed to room temperature, and stirred overnight. To this solution was added, at −78 °C, freshly distilled $PhPBr_2$ (110 μL, 0.53 mmol). The solution was

allowed to warm to room temperature and stirred for 30 h. The solution was filtered on basic alumina (THF) and the volatile materials were removed *in vacuo*. The yellow precipitate of phosphole **2b** ($^{31}P\{^{1}H\}$ NMR (80 MHz, $CDCl_3$): δ = +12.4) was dissolved in THF (20 mL) and AuCl(tht) (169.9 mg, 0.53 mmol) was added to the THF solution and stirred at room temperature overnight. The solvent was removed *in vacuo*. After purification by column chromatography on silica gel (pentane–ether, 1:1) the compound **3b** was obtained as a yellow solid (yield 64%, 280 mg, 0.3 mmol). ^{1}H NMR (200 MHz, CD_2Cl_2): δ = 7.80–7.61 (m, 8 H, 6 $CH_{fluorenyl}$, 2 $CH_{ortho\text{-}phenyl}$), 7.60–7.30 (m, 11 H, 8 $CH_{fluorenyl}$, 3 $CH_{meta\text{-}phenyl}$, $CH_{para\text{-}phenyl}$), 2.96 (m, 4H, $C_{\beta}CH_2$), 1.86 (m, 4H, CH_2), 1.49 (s, 6H, CH_3), 1.46 (s, 6H, CH_3). ^{13}C NMR (50 MHz, $CDCl_3$): δ = 154.0 (s, $C_{fluorenyl}$), 153.9 (s, $C_{fluorenyl}$), 150.3 (d, ^{2}J(P,C) = 17.8 Hz, C_{β}), 139.1 (s, $C_{fluorenyl}$), 138.4 (s, $C_{fluorenyl}$), 134.1 (d, ^{1}J(P,C) = 59.1 Hz, C_{α}), 134.0 (d, ^{2}J(P,C) = 13.7 Hz, $CH_{ortho\text{-}phenyl}$), 132.3 (d, ^{4}J(P,C) = 2.7 Hz, $CH_{para\text{-}phenyl}$), 131.9 (d, ^{2}J(P,C) = 13.6 Hz, $C_{fluorenyl}$), 129.3 (d, ^{3}J(P,C) = 12.1 Hz, $CH_{meta\text{-}phenyl}$), 128.3 (d, ^{3}J(P,C) = 6.5 Hz, $CH_{fluorenyl}$), 127.6 (s, $CH_{fluorenyl}$), 127.1 (s, $CH_{fluorenyl}$), 125.4 (d, ^{1}J(P,C) = 58.0 Hz, C_{ipso}), 123.8 (d, ^{3}J(P,C) = 6.5 Hz, $CH_{fluorenyl}$), 122.6 (s, $CH_{fluorenyl}$), 120.1 (s, $CH_{fluorenyl}$), 120.0 (s, $CH_{fluorenyl}$), 46.8 (s, $C_{fluorenyl}$), 28.6 (s, $C_{\beta}CH_2$), 28.4 (s, $C_{\beta}CH_2$), 26.8 (s, CH_3), 22.6 (s, CH_2). $^{31}P\text{-}\{^{1}H\}$ NMR (80 MHz, CD_2Cl_2): δ = 41.16. Anal. calc. for $C_{44}H_{39}PAuCl$ (831.190): C, 63.58; H, 4.73; P, 3.73; Found: C, 63.92; H, 6.54; P, 4.89.

1-Phenyl-2-(9,9′-dimethylfluorene-2-yl)-5-(phenyl)thiooxophosphole 4a

To a THF solution (10 mL) of Cp_2ZrCl_2 (286 mg, 1.00 mmol) and 1-(9,9′-dimethylfluorene-2-yl)-8-(phenyl)-1,7-octadiyne (366 mg, 1.00 mmol) was added dropwise (*ca.* 1 min), at −78 °C, a hexane solution of *n*-BuLi (2.5 M, 0.8 mL, 2.05 mmol). The solution was warmed to room temperature, and stirred overnight. To this solution was added, at −78 °C, freshly distilled $PhPBr_2$ (0.22 mL, 1.05 mmol). The solution was allowed to warm to room temperature and stirred for 30 h. The solution was filtered on basic alumina (THF) and the volatile materials were removed *in vacuo*. The yellow precipitate containing phosphole **2a** ($^{31}P\{^{1}H\}$ NMR (80 MHz, $CDCl_3$): δ = +11.5) was dissolved in CH_2Cl_2 (20 mL), and elemental sulfur (32 mg, 0.12 mmol) was added to this solution. The reaction mixture was stirred for four days, filtered and the solvent was removed *in vacuo*. After purification on silica gel (*n*-heptane–ethyl acetate, 8:2, v/v, R_f 0.3), **4a** was obtained as a yellow–orange solid (yield = 70%, 0.7 mmol, 360 mg). ^{1}H NMR (300 MHz, CD_2Cl_2): δ = 7.90 (m, 2H, $CH_{ortho\text{-}phenyl}$), 7.72–7.62 (m, 2H, $CH_{fluorenyl}$), 7.55–7.30 (m, 13H, 5 $CH_{fluorenyl}$, 2 $CH_{meta\text{-}phenyl}$, $CH_{para\text{-}phenyl}$, 5 CH_{phenyl}), 2.90 (m, 4H, ≡CCH_2), 1.84 (s, 4H, ≡CCH_2CH_2), 1.44 (s, 6H, CH_3), ^{13}C NMR (75 MHz, CD_2Cl_2): δ = 153.9 (s, $C_{fluorenyl}$), 153.5 (s, $C_{fluorenyl}$), 148.9 (d, ^{2}J(P,C) = 23.1 Hz, C_{β}), 147.9 (d, ^{2}J(P,C) = 23.5 Hz, C_{β}), 138.8 (s, $C_{fluorenyl}$), 138.6 (s, $C_{fluorenyl}$), 134.6 (d, ^{1}J(P,C) = 80.1 Hz, C_{α}), 132.9 (d, ^{2}J(P,C) = 12.9 Hz, $C_{fluorenyl}$), 131.7 (d, ^{1}J(P,C) = 2.7 Hz, $CH_{para\text{-}phenyl}$), 131.6 (d, ^{2}J(P,C) = 11.3 Hz, C_{phenyl}), 130.7 (d, ^{3}J(P,C) = 11.4 Hz, $CH_{ortho\text{-}phenyl}$), 129.1 (d, ^{3}J(P,C) = 5.0 Hz, $CH_{fluorenyl}$), 128.8 (d, ^{3}J(P,C) = 12.2 Hz, $CH_{meta\text{-}phenyl}$), 128.6 (d, ^{1}J(P,C) = 72.5 Hz, C_{ipso}), 128.2 (s, CH_{phenyl}), 127.9 (d, ^{2}J(P,C) = 5.5 Hz, CH_{phenyl}), 127.8 (s, CH_{phenyl}), 127.5 (s, $CH_{fluorenyl}$), 127.0 (s, $CH_{fluorenyl}$), 123.3 (d, ^{3}J(P,C) = 5.3 Hz, $CH_{fluorenyl}$), 122.6 (s, $CH_{fluorenyl}$), 120.1 (s, $CH_{fluorenyl}$), 119.7 (s, $CH_{fluorenyl}$), 46.7 (s, $C_{9\text{-}fluorenyl}$), 28.9 (s, CH_2), 28.8 (s, CH_2), 26.8 (s, CH_3), 26.7 (s, CH_3), 22.8 (s, $C_{\beta}CH_2$), 22.7 (s, $C_{\beta}CH_2$). $^{31}P\{^{1}H\}$ NMR(121 MHz, CD_2Cl_2): δ = 54.01 ppm, *MS* (ESI): m/z 537.17818 (calculated 537.1785 $[M + Na]^+$), m/z 515.19624 (515.1979 $[M + H]^+$). Anal. calc. for $C_{44}H_{39}PS$ (514.672): C, 81.68; H, 6.07; P, 6.02; Found: C, 81.51; H, 6.26; P, 6.32.

1-Phenyl-2,5-bis(9,9′-di(methyl)fluoren-2-yl)thiooxophosphole 4b

A hexane solution of *n*-BuLi (2.5 M, 0.42 mL, 1.06 mmol) was added dropwise (*ca.* 1 min), at −78 °C, to a THF solution (10 mL) of Cp_2ZrCl_2 (155 mg, 0.53 mmol) and 1,8-bis(9,9′-di(methyl)fluorene-2-yl)-1,7-octadiyne (469 mg, 0.53 mmol). The solution was warmed to room temperature, and stirred overnight. To this solution was added, at −78 °C, freshly distilled $PhPBr_2$ (110 μL, 0.53 mmol). The solution was allowed to warm to room temperature and stirred for 30 h. The solution was filtered on basic alumina (THF) and the volatile materials were removed *in vacuo*. The yellow precipitate containing phosphole **2a** ($^{31}P\{^{1}H\}$ NMR (80 MHz, $CDCl_3$): δ = 14.37) was dissolved in CH_2Cl_2 (20 mL), and elemental sulfur (17 mg, 0.07 mmol) was added to this solution. The reaction mixture was stirred for four days, filtered and the solvent was removed *in vacuo*. After purification on silica gel (pentane–CH_2Cl_2, 9:1, v/v, R_f 0.3), **4b** was obtained as a yellow–orange solid (yield = 60%, 200 mg, 0.32 mmol). ^{1}H NMR (300 MHz, CD_2Cl_2): δ = 7.90 (m, 2H, $CH_{ortho\text{-}phenyl}$), 7.72–7.62 (m, 4H, $CH_{fluorenyl}$), 7.50–7.40 (m, 4H, $CH_{fluorenyl}$), 7.43–7.34 (m, 9H, 6 $CH_{fluorenyl}$, 2 $CH_{meta\text{-}phenyl}$, $CH_{para\text{-}phenyl}$), 2.92 (s, 4H, ≡CCH_2), 1.84 (s, 4H, ≡CCH_2CH_2), 1.43 (s, 12H, CH_3). ^{13}C NMR (75 MHz, CD_2Cl_2): δ = 153.1 (s, $C_{fluorenyl}$), 152.8 (s, $C_{fluorenyl}$), 147.5 (d, ^{2}J(P, C) = 23.4 Hz, C_{β}), 138.0 (s, $C_{fluorenyl}$), 137.9 (s, $C_{fluorenyl}$), 133.4 (d, ^{1}J(P, C) = 80 Hz, C_{α}), 131.0 (d, ^{4}J(P,C) = 3.0 Hz, $CH_{para\text{-}phenyl}$), 130.9 (d, ^{2}J(P,C) = 11.9 Hz, $C_{2\text{-}fluorenyl}$), 130.0 (d, ^{3}J(P, C) = 11.3 Hz, $CH_{ortho\text{-}phenyl}$), 128.3 (d, ^{1}J(P, C) = 72.2 Hz, C_{ipso}), 128.0 (d, ^{2}J(P,C) = 12.2 Hz, $CH_{meta\text{-}phenyl}$), 127.2 (d, ^{3}J(P,C) = 5.6 Hz, $CH_{fluorenyl}$), 126.7 (s, $CH_{fluorenyl}$), 126.2 (s, $CH_{fluorenyl}$), 122.6 (d, ^{3}J(P, C) = 5.4 Hz, $CH_{fluorenyl}$) 121.8 (s, $CH_{fluorenyl}$), 119.3 (s, $CH_{fluorenyl}$), 118.6 (s, $CH_{fluorenyl}$), 46.0 (s, $C_{9\text{-}fluorenyl}$), 27.6 (s, CH_2), 27.4 (s, CH_2), 26.1 (s, CH_3), 26.0 (s, CH_3), 22.0 (s, $C_{\beta}CH_2$). $^{31}P\{^{1}H\}$ NMR NMR (120 MHz, CD_2Cl_2): δ = 54.88. MS (ESI): m/z 631.2604 (calculated 631.2588, $[M + H]^+$), m/z 653.3406 (calculated 653.2408, $[M + Na]^+$). Anal. calc. for $C_{44}H_{39}PS$ (630.835): C, 83.78; H, 6.23; P, 4.91; Found: C, 83.92; H, 6.54; P, 4.89.

Acknowledgements

This work is supported by the Ministère de la Recherche et de l'Enseignement Supérieur, the Institut Universitaire de France, the CNRS, the Région Bretagne, and the project

ANR PSICO. Thanks are due to Dr Christophe Lescop and Dr Dimitri Aldakov for X-ray diffraction studies and fluorescence measurements of PMMA films, respectively.

References

1 (*a*) *Organic Light Emitting Devices: Synthesis Properties and Applications*, ed. K. Müllen and U. Scherf, Wiley-VCH, Weinheim, Germany, 2006; (*b*) K. Müllen and G. Wegner, *Electronic Materials: The Oligomer Approach*, Wiley-VCH, Weinheim, 1998; (*c*) T. A. Skotheim, R. L. Elsenbaumer and J. R. Reynolds, *Handbook of Conducting Polymers*, Dekker, New York, 2nd edn, 1998.

2 (*a*) G. Ramakrishna, A. Bhaskar, P. Bauerle and T. Goodson III, *J. Phys. Chem. A*, 2008, **112**, 2018; (*b*) S. Yamaguchi and K. Tamao, *Chem. Lett.*, 2005, **34**, 2; (*c*) G. Gotz, S. Scheib, R. Klose, J. Heinze and P. Bauerle, *Adv. Funct. Mater.*, 2002, **12**, 723; (*d*) M. Hissler, R. Réau and P. Dyer, *Coord. Chem. Rev.*, 2003, **244**, 1; (*e*) J. Roncali, *Chem. Rev.*, 1997, **97**, 173.

3 (*a*) Y. Matano and H. Imahori, *Org. Biomol. Chem.*, 2009, **7**, 1258; (*b*) A. Fukazawa and S. Yamaguchi, *Chem.–Asian J.*, 2009, **4**, 1386; (*c*) R. Réau and T. Baumgartner, *Chem. Rev.*, 2007, **107**, 303; (*d*) M. Hobbs and T. Baumgartner, *Eur. J. Inorg. Chem.*, 2007, 3611; (*e*) F. Mathey, *Chem. Rev.*, 1988, **88**, 429; (*f*) U. Salzner, J. B. Lagowski, P. G. Pickup and R. A. Poirier, *Synth. Met.*, 1998, **96**, 177; (*g*) J. Ma, S. Li and Y. Jiang, *Macromolecules*, 2002, **35**, 1109; (*h*) D. Delaere, A. Dransfeld, M. N. Nguyen and L. G. Vanquickenborne, *J. Org. Chem.*, 2000, **65**, 2631.

4 (*a*) F. Mathey, *Phosphorus-Carbon Heterocyclic Chemistry: The Rise of a New Domain*, ed. Elsevier Science Ltd., Oxford, 2001; (*b*) K. Dillon, F. Mathey and J. F. Nixon, *Phosphorus: The Carbon Copy*, John Wiley and Sons Ltd., Chichester, 1998; (*c*) L. Nyulaszi, *Chem. Rev.*, 2001, **101**, 1229; (*d*) E. Mattmann, F. Mathey, A. Sevin and G. Frisson, *J. Org. Chem.*, 2002, **67**, 1208.

5 (*a*) C. Hay, M. Hissler, C. Fischmeister, J. Rault-Berthelot, L. Toupet, L. Nyulászi and R. Réau, *Chem.–Eur. J.*, 2001, **7**, 4222; (*b*) C. Fave, T.-Y. Cho, M. Hissler, C.-W. Chen, T.-Y. Luh, C.-C. Wu and R. Réau, *J. Am. Chem. Soc.*, 2003, **125**, 9254; (*c*) C. Hay, C. Fave, M. Hissler, J. Rault-Berthelot and R. Réau, *Org. Lett.*, 2003, **5**, 3467; (*d*) C. Fave, M. Hissler, T. Kárpáti, J. Rault-Berthelot, V. Deborde, L. Toupet, L. Nyulászi and R. Réau, *J. Am. Chem. Soc.*, 2004, **126**, 6058; (*e*) H.-C. Su, O. Fadhel, C.-J. Yang, T.-Y. Cho, C. Fave, M. Hissler, C.-C. Wu and R. Réau, *J. Am. Chem. Soc.*, 2006, **128**, 983.

6 (*a*) E. Deschamps, L. Ricard and F. Mathey, *Angew. Chem., Int. Ed. Engl.*, 1994, **33**, 1158; (*b*) Y. Matano, M. Nakashima and H. Imahori, *Angew. Chem., Int. Ed.*, 2009, **48**, 4002.

7 N. H. T. Huy, B. Donnadieu, F. Mathey, A. Muller, K. Colby and C. J. Bardeen, *Organometallics*, 2008, **27**, 5521.

8 K. Shiraishi, T. Kashiwabara, T. Sanji and M. Tanaka, *New J. Chem.*, 2009, **33**, 1680; T. Sanji, K. Shiraishi and M. Tanaka, *ACS Appl. Mater. Interfaces*, 2009, **1**, 270.

9 (*a*) H. S. Na, Y. Morisaki, H. Na, Y. Aiki and Y. Chujo, *Polym. Bull.*, 2007, **58**, 777; (*b*) H. S. Na, Y. Morisaki, Y. Aiki and Y. Chujo, *J. Polym. Sci., Part A: Polym. Chem.*, 2007, **45**, 2867; (*c*) H.-S. Na, Y. Morisaki, Y. Aiki and Y. Chujo, *Polym. Bull.*, 2007, **58**, 645.

10 (*a*) A. Fukazawa, M. Hara, T. Okamoto, E. C. Son, C. Xu, K. Tamao and S. Yamaguchi, *Org. Lett.*, 2008, **10**, 913; (*b*) A. Fukazawa, I. Aiko, K. Yasunori, Y. Kosaka and S. Yamaguchi, *Chem.–Asian J.*, 2009, **4**, 1729.

11 (*a*) Y. Dienes, S. Durben, T. Karpati, T. Neumann, U. Englert, L. Nyulaszi and T. Baumgartner, *Chem.–Eur. J.*, 2007, **13**, 7487; (*b*) T. Baumgartner, T. Neumann and B. Wirges, *Angew. Chem., Int. Ed.*, 2004, **43**, 6197; (*c*) Y. Dienes, U. Englert and T. Baumgartner, *Z. Anorg. Allg. Chem.*, 2009, **635**, 238; (*d*) C. R. Nieto, S. Durben, I. M. Kormos and T. Baumgartner, *Adv. Funct. Mater.*, 2009, **19**, 3625.

12 (*a*) Y. Matano, T. Miyajima, T. Fukushima, H. Kaji, Y. Kimura and H. Imahori, *Chem.–Eur. J.*, 2008, **14**, 8102; (*b*) Y. Matano, T. Miyajima, H. Imahori and Y. Kimura, *J. Org. Chem.*, 2007, **72**, 6200.

13 (*a*) C. W. Tang and S. A. Vanslyke, *J. Appl. Phys.*, 1987, **51**, 913; (*b*) C. W. Tang, S. A. Vanslyke and C. H. Chen, *J. Appl. Phys.*, 1989, **65**, 3610; (*c*) J. H. Burroughes, D. D. C. Bradley, A. R. Brown, R. N. Marks, K. Mackay, R. H. Friends, P. L. Burns and A. B. Holmes, *Nature*, 1990, **347**, 539; (*d*) A. A. Arias, J. D. Mackenzie, I. McCulloch, J. Rivnay and A. Salleo, *Chem. Rev.*, 2010, **110**, 3; (*e*) A. C. Grimsdale, K. L. Chan, R. E. Martin, P. G. Jokisz and A. B. Holmes, *Chem. Rev.*, 2009, **109**, 897.

14 H. Tsuji, K. Sato, Y. Sato and E. Nakamura, *J. Mater. Chem.*, 2009, **19**, 3364.

15 R. Chen, R. Zhu, Q. Fan and W. Huang, *Org. Lett.*, 2008, **10**, 2913.

16 O. Fadhel, M. Gras, N. Lemaitre, V. Deborde, M. Hissler, B. Geffroy and R. Reau, *Adv. Mater.*, 2009, **21**, 1261.

17 (*a*) P. J. Fagan and W. A. Nugent, *J. Am. Chem. Soc.*, 1988, **110**, 2310; (*b*) P. J. Fagan, W. A. Nugent and J. C. Calabrese, *J. Am. Chem. Soc.*, 1994, **116**, 1880; (*c*) X. Sava, N. Mézaille, N. Maigrot, F. Nief, L. Ricard, F. Mathey and P. Le Floch, *Organometallics*, 1999, **18**, 4205; (*d*) E. Negishi and T. Takahashi, *Acc. Chem. Res.*, 1994, **27**, 124; (*e*) T. Takahashi, F.-Y. Tsai, Y. Li, K. Nakajima and M. Kotora, *J. Am. Chem. Soc.*, 1999, **121**, 11093.

18 J. C. de Mello, H. F. Wittmann and R. H. Friend, *Adv. Mater.*, 1997, **9**, 230.

19 J. Jo, C. Chi, S. Höger, G. Wegner and D. Y. Yoon, *Chem.–Eur. J.*, 2004, **10**, 2681.

20 Z. Zhao, Z. Wang, P. Lu, C. Y. K. Chan, D. Liu, J. W. Y. Lam, H. H. Y. Sung, I. D. Williams, Y. Ma and B. Z. Tang, *Angew. Chem., Int. Ed.*, 2009, **48**, 7608.

21 Y. Zhu, R. D. Champio and S. A. Jenekhe, *Macromolecules*, 2006, **39**, 8712.

22 Z. Otwinowski and W. Minor, in *Methods in Enzymology*, ed. C. W. Carter, Jr. and R. M. Sweet, Academic Press, New York, 1997, vol. 276, p. 307.

23 A. Altomare, M. C. Burla, M. Camalli, G. Cascarano, C. Giacovazzo, A. Guagliardi, A. G. G. Moliterni, G. Polidori and R. Spagna, *J. Appl. Crystallogr.*, 1999, **32**, 115.

24 G. M. Sheldrick, *SHELX97*, Program for the Refinement of Crystal Structures, University of Göttingen, Germany, 1997.

25 International Tables for X-ray Crystallography, vol. C, Kluwer, Dordrecht, 1992.

26 L. D. Quin, J. P. Gratz and T. P. Barket, *J. Org. Chem.*, 1968, **33**, 1034.

27 S. Liu, Q. Zhao, R. Chen, Y. Deng, Q. Fan, F. Li, L. Wang, C. Huang and W. Huang, *Chem.–Eur. J.*, 2006, **12**, 4351.

28 H. D. Kaesz, *Inorg. Synth.*, 1989, **26**, 86.

29 J. Chen, C. C. W. Law, J. W. Y. Lam, Y. Dong, S. M. F. Lo, I. D. Williams, D. Zhu and B. Z. Tang, *Chem. Mater.*, 2003, **15**, 1535.

30 J. N. Demas and G. A. Crosby, *J. Phys. Chem.*, 1971, **75**, 991.